

# Infrared Absorption by Ferroelectric Thin-Film Structures

July 1998

W. A. Beck, Robert C. Hoffman, Dale N. Robertson, Meimei Z. Tidrow, C. Wesley Tipton,  
and William W. Clark III  
Army Research Laboratory  
Adelphi, MD

H.R. Beratan, K.R. Udayakumar, Kevin Soch, and C.M. Hanson  
Raytheon Systems  
Dallas, TX

## ABSTRACT

Infrared absorbing, air-bridge, structures are anticipated to be used in the next generation of ferroelectric uncooled infrared detectors. These structures will consist of resonant cavities with an absorbing bridge element, which contains the ferroelectric detector and the contact electrodes. It is desired to use an oxide electrode rather than a metallic electrode, as the metallic electrode reflects too much of the incoming radiation at reasonable thickness. For this paper, spectral transmission and reflection of LSCO films was measured and it was found that the properties could be described as a simple two-dimensional conducting sheet. The optical absorption of several air-bridge structures was modeled, and optimized dimensions and electrode conductivity are presented which yield greater than 80% absorption over the full 8-14  $\mu\text{m}$  band.

## 1. Introduction

Uncooled infrared focal plane arrays composed of thin-film ferroelectric (FE) detecting elements show great promise for low-cost infrared imaging with projected temperature sensitivity below 10 mK with  $f/1$  optics. To achieve high optical absorption with low thermal mass, air-bridge structures will be used in which optical resonance between the FE layer and the underlying read-out integrated circuit (ROIC) is used to enhance absorption over the 8 to 14  $\mu\text{m}$  long wavelength infrared (LWIR) spectral band.

As shown in Figure 1(a), the simplest resonant absorption structure consists of a conducting film with sheet resistivity equal to the free-space impedance  $Z_0 = 120\pi \Omega$ , spaced one-fourth of a wavelength ( $\lambda/4$ ) above the reflecting surface. Such a structure has a theoretical absorption of 100 percent at the

design wavelength. The desired detector/ROIC is more like the structure shown in Figure 1(b). It includes a finite-thickness FE element with conducting electrodes on both sides suspended over the ROIC.

Early versions of the thin-film FE pixel structure at Raytheon have used a 3000-Å-thick FE layer with a thick opaque platinum electrode and a semitransparent NiCr front electrode. This pixel structure was used to maximize process yield in early devices although, as shown later, the optical absorption is lower than will be achieved in structures with semitransparent front and back electrodes.

In this paper, we have measured the optical transmission and reflection of a promising semitransparent electrode material, lanthanum-strontium-cobalt-oxygen (LSCO). We also have determined optimum values for the electrode conductivity and FE-ROIC cavity spacing to maximize the absorption of the actual detector structure at a specified wavelength and computed the absorption spectrum over the LWIR band.

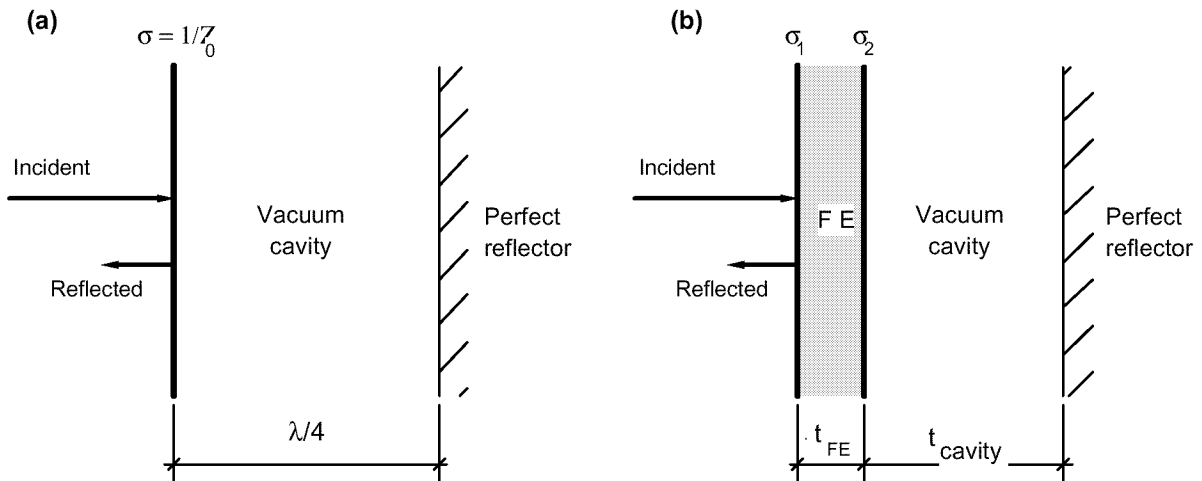


**Figure 1: Optical absorption structures: (a) Simple  $\lambda/4$  structure and (b) actual detector structure with ferroelectric (FE) layer, electrodes ( $\sigma_1$  and  $\sigma_2$ ), and vacuum cavity over perfectly conducting ROIC.**

## 2. Procedure

### 2.1. LSCO Growth

The LSCO films were deposited on the Si substrates using a KrF pulsed-eximer laser deposition (PLD) system. The substrate heater temperature was maintained at 500 to 550° C during the deposition. All depositions were performed in an O<sub>2</sub> environment at 10 mTorr. Spectroscopic observations showed that under these conditions no oxidation of the Si substrate occurred.

### 2.2. Model

The reflection from (and therefore absorption in) the structure was computed using a 2 x 2 transfer matrix formulation.<sup>1</sup> The FE layer was assumed to have an isotropic refractive index of  $n = 2.24$  and no absorption for most calculations. The effect of varying  $n$  between 2.1 and 2.5<sup>2</sup> was also determined for

some results. The surface of the ROIC was assumed to be a perfectly reflecting mirror. The electrodes were approximated as thin (two-dimensional) sheets with specified sheet conductivity.

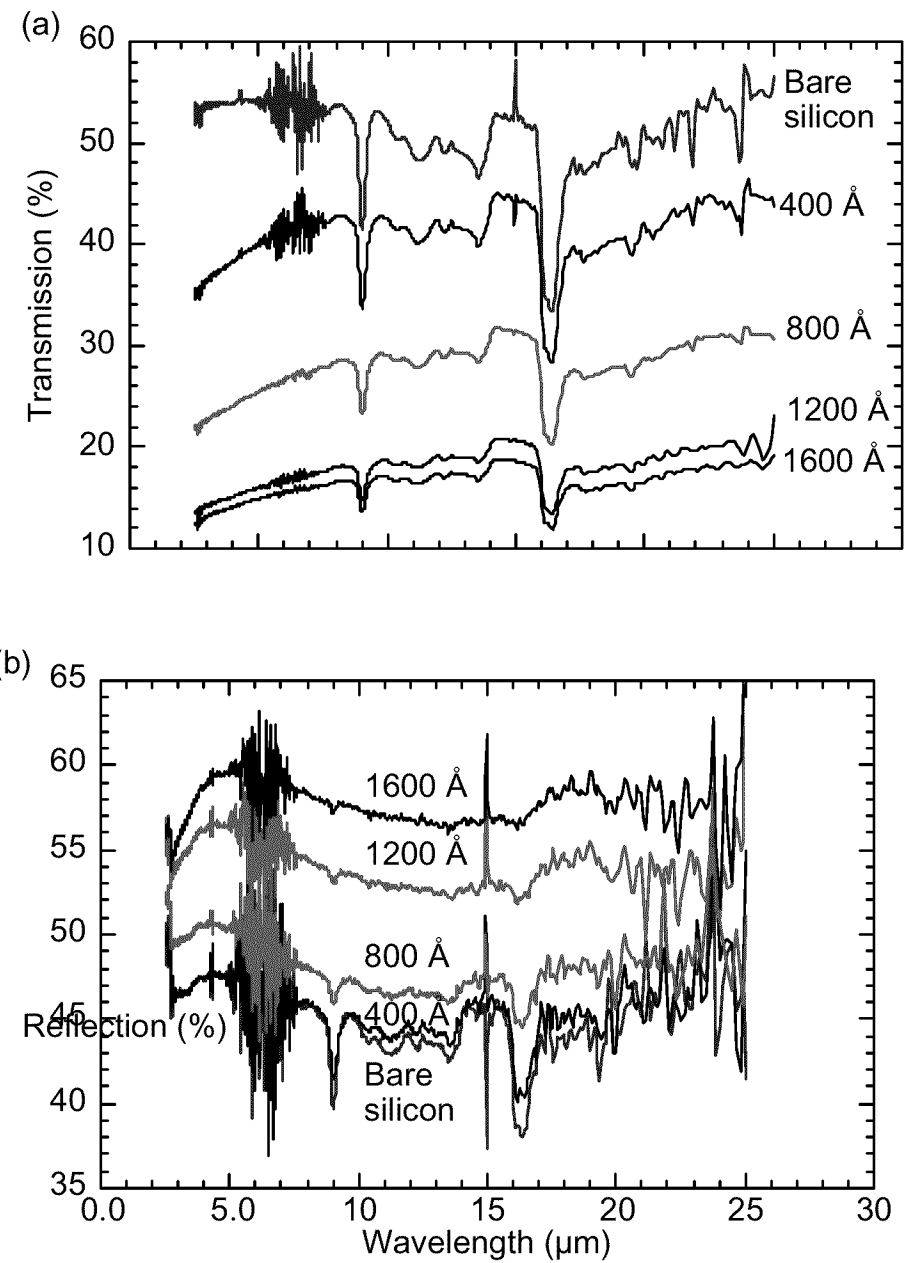
### 3. Results

#### 3.1. LSCO Measurements

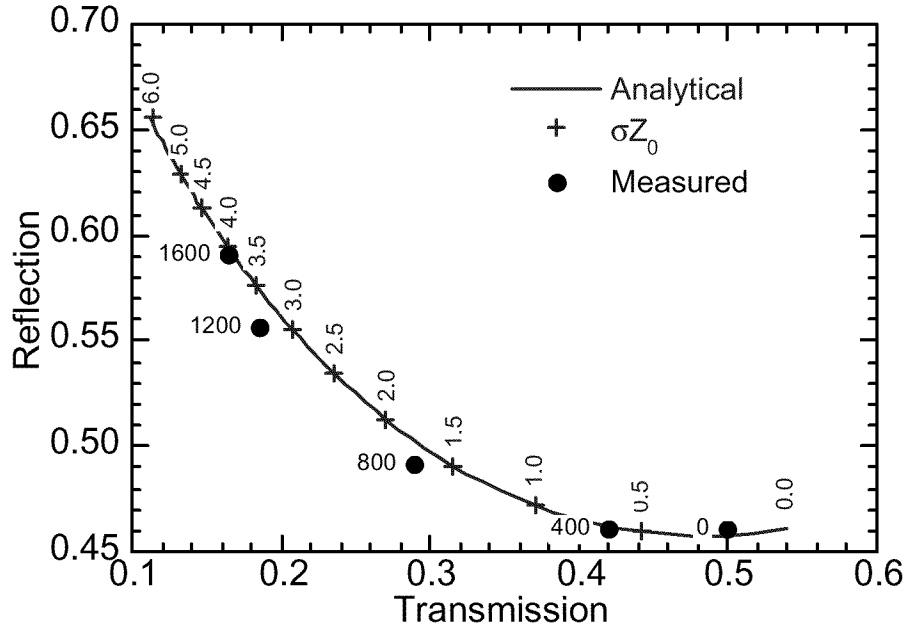
Figure 2 shows the measured transmittance and reflectance for several thicknesses of LSCO on a Si substrate. To interpret these measurements, we computed the expected transmission and reflection for a two-dimensional conducting layer on a Si substrate as a function of the layer conductivity. Because no interference fringes from the Si substrate were observed, presumably due to small thickness variations, we assumed that reflections from the two Si surfaces were incoherent.

Figure 3 shows the analytical result along with the measured values extracted (as approximate average values in the LWIR band) from the data in Figure 1. That the measured values follow the analytical curve indicates that the LSCO optical properties in the LWIR region are adequately described as a simple two-dimensional conducting sheet.

Figure 4 shows the  $\sigma Z_0$  and sheet  $\sigma$  implied by Figure 3 versus the LSCO thickness. The sheet conductivity increases approximately linearly, with film thickness corresponding to a bulk resistivity of 1.55 mΩ-cm. This is comparable to the value of 1.95 mΩ-cm that was measured on similar films (deposited on SiO<sub>2</sub>-buffered insulating Si substrates) using a dc four-point probe. Because the dc and optical measurements were performed on different samples, it is uncertain whether the small difference in resistivity is significant.



**Figure 2:** (a) Transmission and (b) reflection for LSCO layers on Si substrate. LSCO thickness is indicated.



**Figure 3:** Reflection vs. transmission for two-dimensional conducting layer on Si substrate. Solid line is analytical result, bullets are from measured data in Figure 1, and crosses indicate  $\sigma Z_0$  corresponding to analytical result.

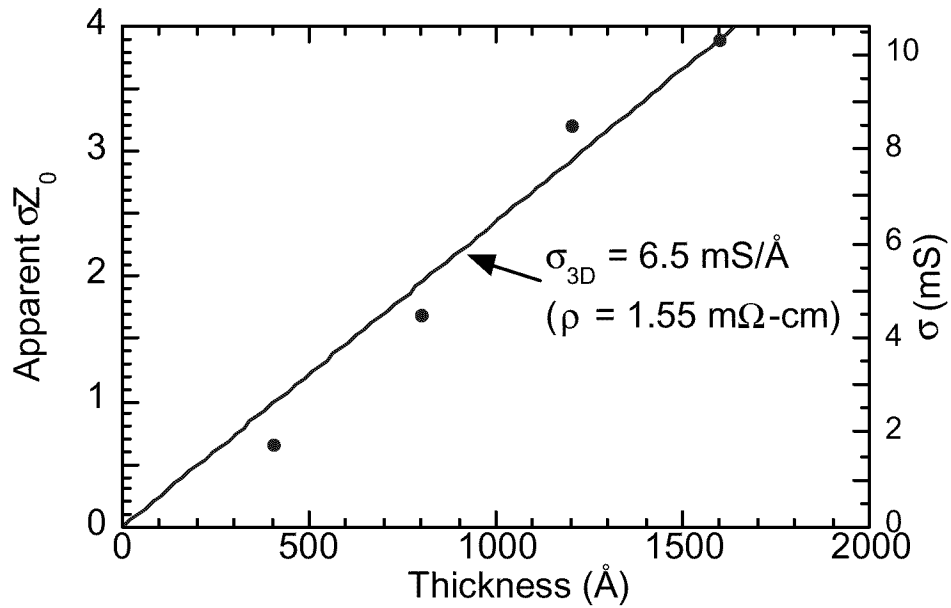


**Figure 4:** Apparent value of  $\sigma Z_0$  (left axis) and corresponding sheet conductivity (right axis) from Figure 3 vs. LSCO thickness. Solid line is linear fit indicating bulk conductivity and resistivity.

### 3.2. Detector Modeling

#### 3.2.1. Simple $\lambda/4$ Structure

For comparison to other results, the absorption spectrum of a simple  $\lambda/4$  structure (Figure 1(a)) that was optimized for a wavelength of  $11\text{ }\mu\text{m}$  is shown in Figure 5. Note that the absorption is greater than 90 percent over the full LWIR band.

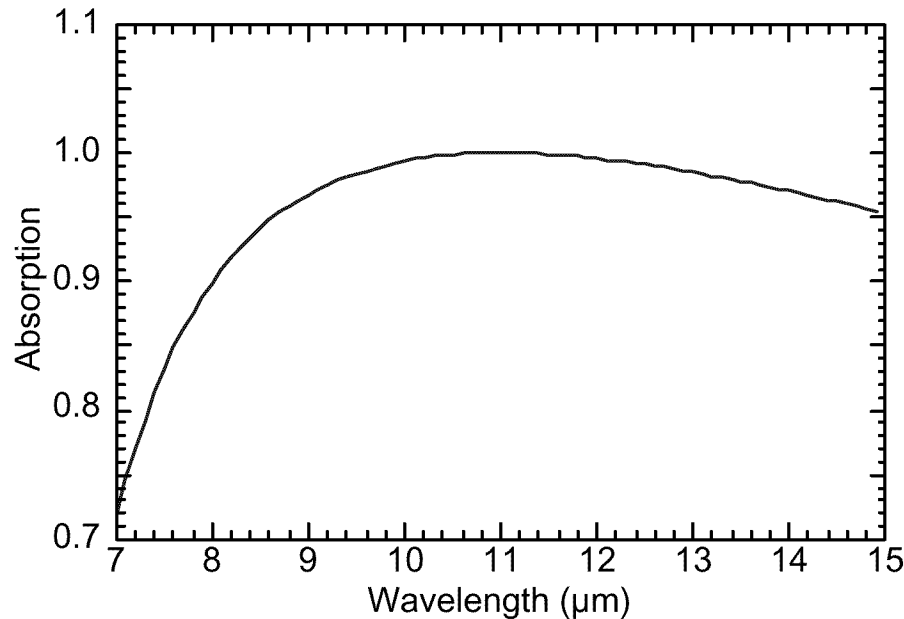


**Figure 5: Absorption spectrum for simple  $\lambda/4$  cavity structure optimized for  $\lambda = 11\text{ }\mu\text{m}$ .**

#### 3.2.2. Semitransparent Front Electrode With Opaque Back Electrode

As mentioned previously, early devices use an opaque back electrode and semi-transparent front electrode on a 3000-Å-thick FE layer. shows the computed absorption spectra for the structure. The spectra were computed for a front-electrode conductivity of  $1/Z_0$ , and also for a more optimized front-electrode conductivity of  $5.5/Z_0$ . The FE layer is too thin to form an optimum cavity; therefore the absorption is limited to 20 to 40 percent over the LWIR band, even with optimized electrode conductivity.

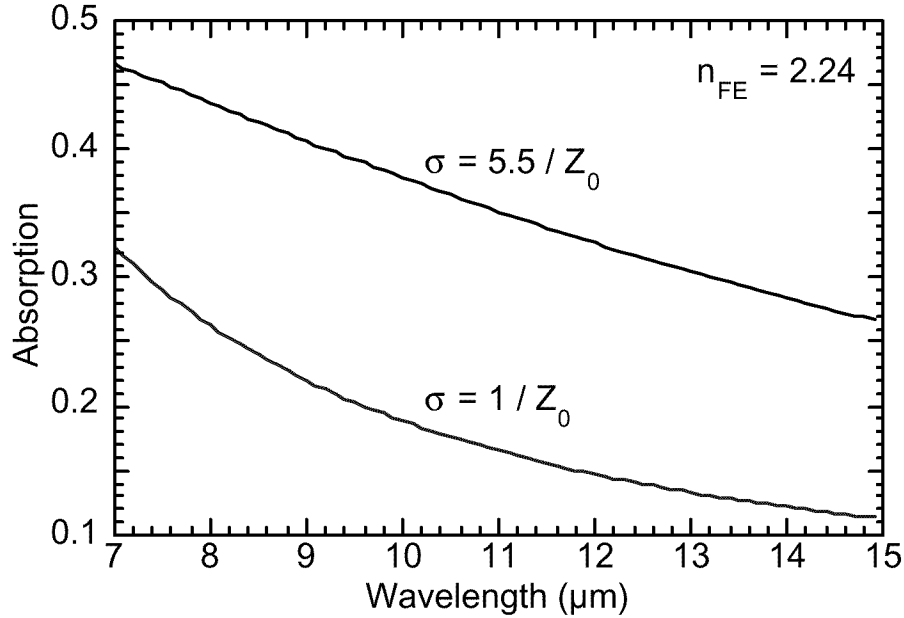


**Figure 6: Absorption spectrum for a 3000-Å-thick FE structure with opaque back electrode and front electrode with  $\sigma = 1/Z_0$  and  $5.5 / Z_0$ .**

### 3.2.3. Front and Back Semitransparent Electrodes

The desired detector structure has semitransparent front *and* back electrodes. It is possible to separately optimize the conductivity of each electrode; however, it will generally be desirable to have equal sheet conductivity in both electrodes. Otherwise the resistance of the less conductive electrode will dominate the electrical resistance and Johnson noise of the detector. Furthermore, as shown below, it is possible to achieve nearly 100 percent absorption (at a single wavelength) in an optimized structure with equal-conductivity electrodes.

For the following figures, we assumed a structure with adjustable cavity spacing and a FE layer with thickness specified between 0 and 5000 Å that was surrounded by equal-conductivity electrodes. For each FE thickness, the electrode conductivity and cavity spacing were varied to achieve maximum absorption at a wavelength of 11 μm. It turned out that an absorption of 100 percent was obtained at all FE thicknesses. The optimum values are shown in Figure 7 for three different values of the FE refractive index. Note that in the limit of FE thickness = 0, the optimum conductivity is  $0.5/Z_0$  and the optimum cavity thickness is  $11 \mu\text{m}/4$ , which is consistent with a simple  $\lambda/4$  cavity structure because the two electrodes merge to form a single electrode with conductivity of  $1/Z_0$ .

The corresponding absorption spectra are shown in Figure 8. Note that although all structures achieve 100 percent absorption at 11 μm, the integrated absorption over the LWIR band is somewhat lower for thicker FE layers.

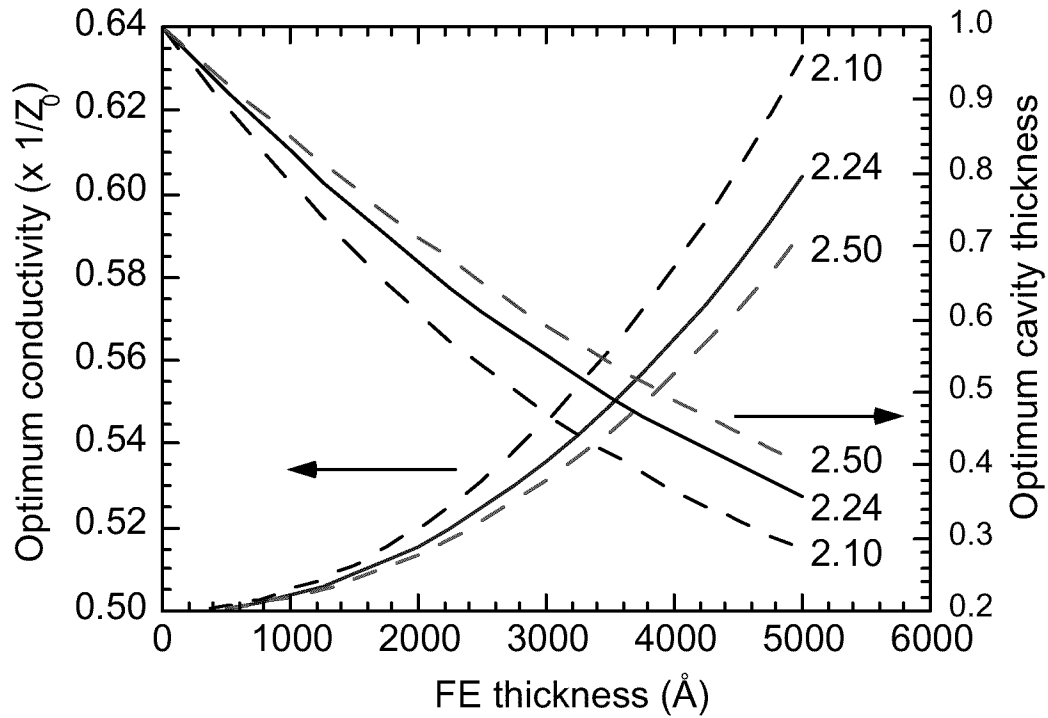


**Figure 7: Optimum electrode sheet conductivity ( $\times 1/Z_0$ ) and cavity thickness vs. FE thickness. Cavity thickness of 1.0 is  $11\mu\text{m} / 4$ . Refractive index of FE is indicated for each curve.**

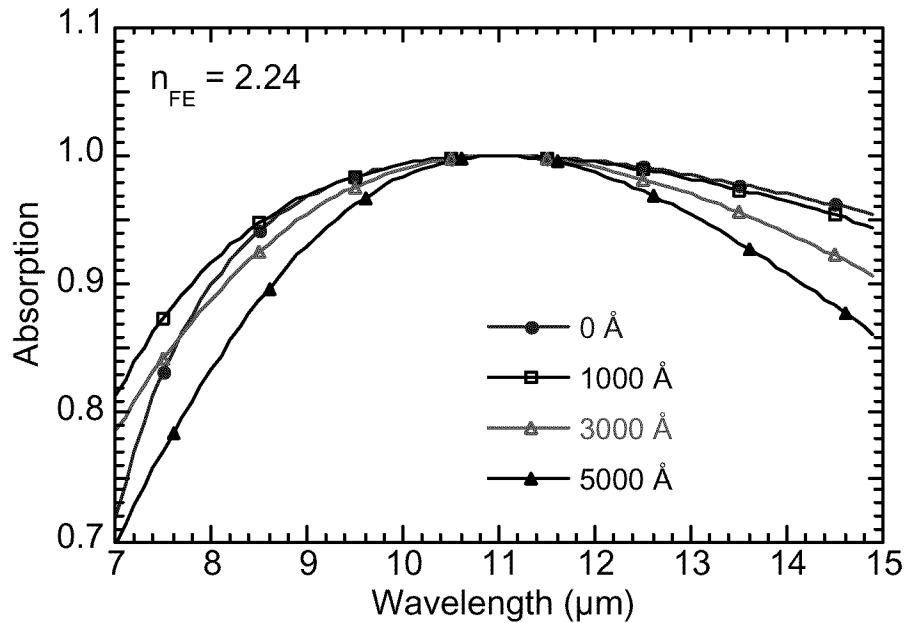


**Figure 8: Calculated absorption spectra at several FE thicknesses using optimized parameters from Figure 7.**

### 3.2.4. Blackbody Source With $f/1$ Illumination

The results presented so far were for illumination perpendicular to the detector. However, the actual illumination in most uncooled systems would come from an  $f/1$  objective. Therefore we computed the absorption for a weighted average over incident angles corresponding to the  $f/1$  objective and also averaged over the spectrum of incident power between 8 and 14  $\mu\text{m}$  corresponding to a 300-K blackbody.

The optimum electrode conductivity and cavity thickness were first determined for a structure with equal-conductivity electrodes and a FE layer thickness of 3000  $\text{\AA}$ . It turned out that the optimum values to achieve maximum integrated absorption ( $\sigma = 0.562 / Z_0$ ,  $t = 1.594 \mu\text{m}$ ) were only slightly different from the values to achieve maximum normal-incidence absorption at a wavelength of 11  $\mu\text{m}$  ( $\sigma = 0.536 / Z_0$ ,  $t = 1.507 \mu\text{m}$ ). We then determined the change in total integrated absorption that resulted from deviations from the optimum values. The results (Figure 9) show that it is possible (within the approximations of the present model) to absorb 97.2 percent of LWIR radiation from the  $f/1$  objective. Furthermore, the absorption is relatively insensitive to variations in the electrode conductivity and cavity thickness near the optimum point.

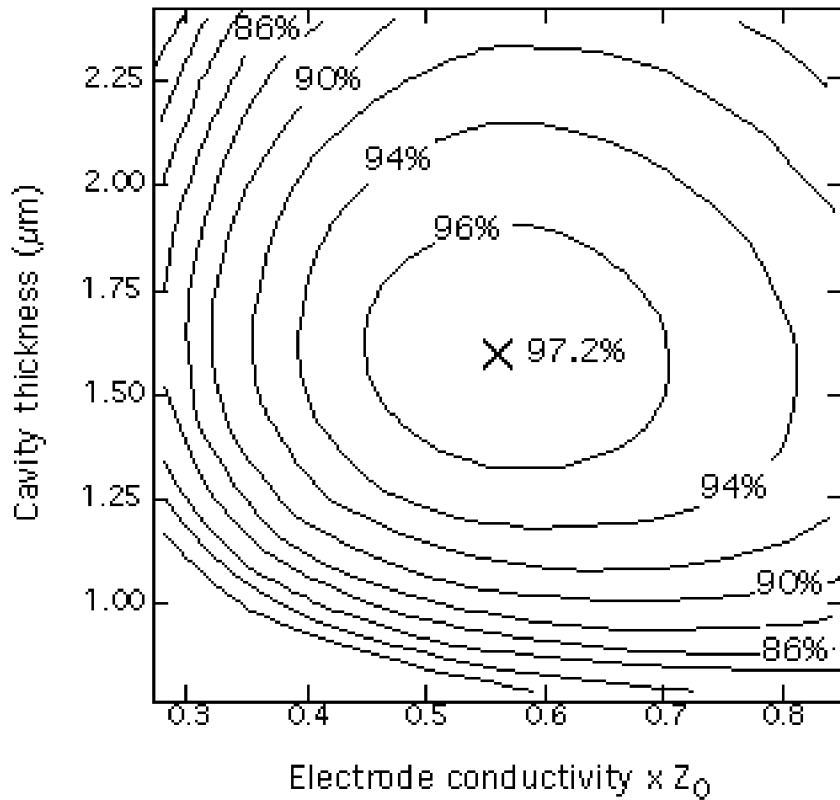


**Figure 9: Calculated fraction of incident light absorbed from 300-K blackbody source between 8 and 14  $\mu\text{m}$ . Incident angles simulate an  $f/1$  objective. FE layer thickness is 3000  $\text{\AA}$ .**

## 4. Conclusions

Transmission and reflection measurements indicate that the optical properties of LSCO layers up to 1600-Å thick can be described by a simple two-dimensional conducting sheet whose sheet conductivity increases linearly with film thickness. The bulk resistivity implied by the optical measurements (1.55 mΩ-cm) was comparable to the resistivity determined from four-point probe measurements (1.95 mΩ-cm). These values for as-grown, laser-ablated films are comparable to those previously observed in sputtered LSCO that had been post-growth annealed for 30 to 60 seconds at 650 C.

A multilayer optical model was used to calculate the expected optical absorption for several important thin-film FE structures, approximating the LSCO semitransparent electrodes as two-dimensional conducting layers. The structure using an opaque back electrode on a 3000-Å-thick ferroelectric is limited to absorption of 20 to 40 percent over the LWIR band.

On the other hand, an optimized structure using equivalent semitransparent front and back electrodes and a vacuum cavity behind the FE layer should have normal-incidence absorption near 100 percent at the design wavelength, and integrated absorption of up to 97 percent of the LWIR power from an  $f/1$  objective. The optimum electrode conductivity of  $\sim(0.5 \text{ to } 0.6) / Z_0$  corresponds to a thickness of around 250 Å for the LSCO films measured for this paper, which is a practical thickness for real detectors.

## 5. References

- 1 P. Yeh, *Optical Waves in Layered Media* (John Wiley & Sons, New York, 1988).
- 2 G. H. Haertling, J. American Ceramic Society **54**, 303-309 (1971).